STRUCTURAL CHARACTERISTICS OF CONCRETE-FILLED GLASS FIBER REINFORCED COMPOSITE PILES

Sung Woo Lee[1], Sokhwan Choi[2], Byung-Suk Kim[3], Young-Jin Kim[4], Sung-Yong Park[5]

[1]*Prof., Dept of Civil & Environmental Eng., Kookmin University, Seoul, Korea*
[2]*Assistant Prof., Dept of Civil & Environmental Eng., Kookmin University, Seoul, Korea*
[3]*Director, Structural System Group, Korea Institute of Construction Technology, Ilsan, Korea*
[4]*Senior Researcher, Structural System Group, Korea Institute of Construction Technology, Ilsan, Korea*
[5]*Researcher, Structural System Group, Korea Institute of Construction Technology, Ilsan, Korea*

Abstract

Concrete-filled glass fiber reinforced polymer piles(GFRP piles) have been introduced to overcome the corrosion problems associated with concrete and steel piles under severe environments. Benefits of composite piles include high durability, high confined strength, low maintenance cost, high ductility, and long expected service life. Current research has been carried out to examine material and structural characteristics of GFRP piles. It includes the compression test for short-length composite tubes, axial-flexure test under various load combinations, buckling test with several different slenderness ratios. Besides, large-scale piles were tested to investigate the flexural and bond characteristics. Experiments showed that the inside spirals increase the bond and improve the whole flexure behavior. Numerical procedure to construct P-M diagrams for composite piles were also developed and the results were compared with experiments. Present study will demonstrate the applicability of concrete-filled glass fiber reinforced composite piles as an alternative to conventional steel or concrete piles in corrosive environments, and provide an experimental database about the multidirectionally reinforced composite piles.

KEYWORDS: GFRP, Composite pile, Glass fiber, Flexure-Compression test, Slenderness

Introduction

The research described in this paper deals with the behavior of concrete-filled composite tubes that are often used as marine piles. Many researches about FRP (fiber reinforced plastics) composite tubes have been introduced to resolve the corrosion and deterioration issues of steel and concrete piles under harmful environments[1-6]. A deteriorated pile is shown in Figure 1. High strength obtained under confinement, low maintenance cost, high ductility, and long expected service life are some benefits of composite piles we can mention. In the current study, concrete-filled GFRP piles were fabricated and tested under uni-axial compression, pure bending, and axial-flexure in oder to examine fabrication process, and investigate the structural characteristics. Slenderness effect was also examined with various pile lengths. Some large scale piles were tested under flexure and the importance of bond action between the concrete and composite shells was confirmed.

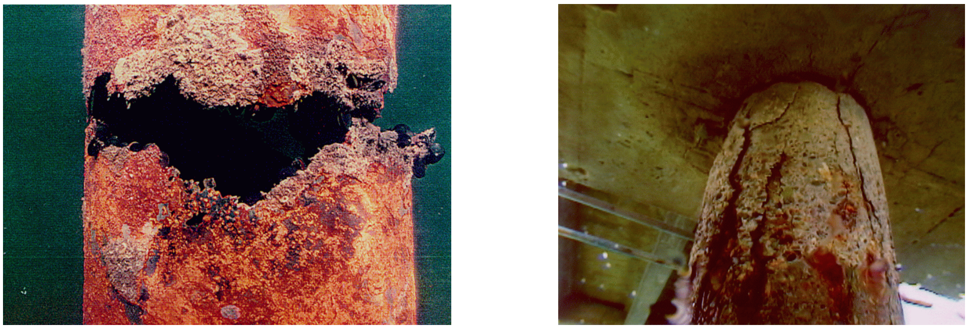

Figure 1. Deterioration observed at steel (left) and concrete (right) piles

Table 1. Properties of composite tubes

Properties		Value
Layer		L900-5PLY FW-2PLY
Fiber volume for HL (%)		35
Fiber volume for FW (%)		50
Ply thickness	0^{o}	4.85
	90^{o}	1.82
Total tube thickness (mm)		6.7
Inner diameter (mm)		165.2
E_x of tube (MPa)		2.32×10^4
E_y of tube (Mpa)		1.73×10^4
G_{xy} of tube (MPa)		4.76×10^3
ν_{xy} of the tube		0.22

Experimental tasks and analytical work

Uni-axial compression test for concrete-filled composite tubes

Properties of shells and dimensions of piles are given in Table 1. These layouts were used for the following three tests: 1) uni-aixal compression test, 2) pure bending test, 3) axial-flexure test. FRP shells were optimized to efficiently resist to both compressive and bending stresses. The composite shells must have orthotropic plies to provide both axial and transverse reinforcement. The filled-in concrete in the tube had a design strength of 40MPa at 28 days. Composite piles give much higher strength and ductility comparing with plain concrete specimens due to confinement action of the tubes.

Five specimens of concrete-filled GFRP tubes with L/D=2 were tested under uni-axial compression using material testing machine that has the capacity of 4.9MN (Figure 2). Load was applied under displacement control with the loading rate of 0.5 mm/min. Strain gages were attached at the middle part of the member in both the axial and circumferential directions. Figure 3 shows the stress-strain curves in axial direction, and both curves in axial and lateral directions can be seen in Figure 4. Labels s-1 ~ s-4 in the figure simply represent specimen ID. It is recognized that the stress-strain response can be divided into two parts; first part showing high stiffness, and second part revealing high ductility due to confinement effect. The strengths of the concrete-filled FRP tubes were 2.0 ~ 2.4 times higher than those of plain concrete cylinders. The strains at failure were also 5.3 ~ 7.0 times higher for FRP tubes revealing high ductility.

Figure 2. Test setup under compression for concrete-filled short composite tubes

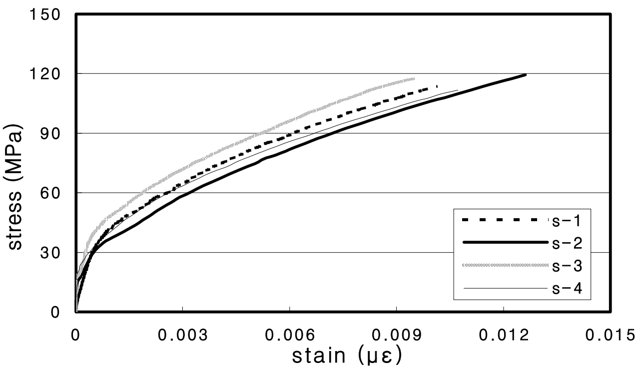

Figure 3. Stress-strain curves in axial direction

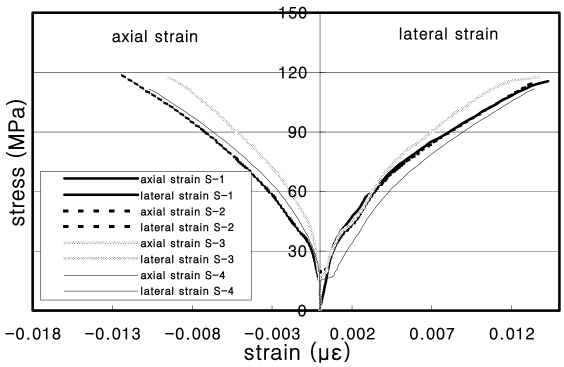

Figure 4. Strains in axial and lateral directions

Pure flexural and axial-flexural test

Two FRP tubes were tested under pure flexure (PF-1, PF-2; diameter=165mm, span=1200mm) as shown in Figure 5. Figure 6 is the relation between the applied moments and strains at the top and bottom faces at the middle of the span. Seven members were tested under axial-flexure load (P-1 through P-7; diameter=165mm, span=1200mm). After predetermined axial load was applied first, flexural force was applied. Initial axial force and final moments at failure are given in Table 2. Tension failure was induced for test member P-1 through P-5, and compression failure was developed in P-6 and P-7. Load-displacement curves at the bottom of mid-span were given in Figure 7.

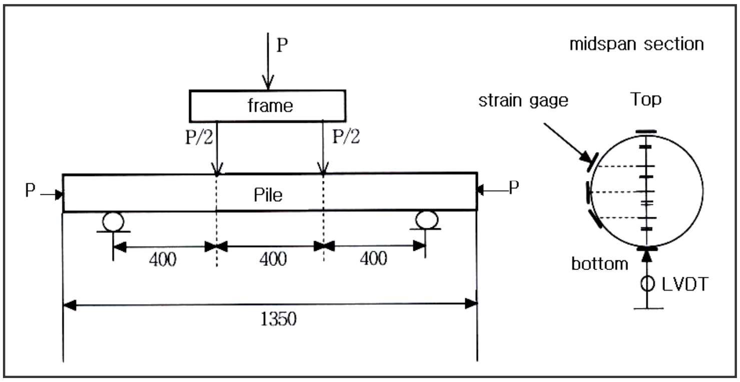

Figure 5. Pure flexural and axial-flexural test setup

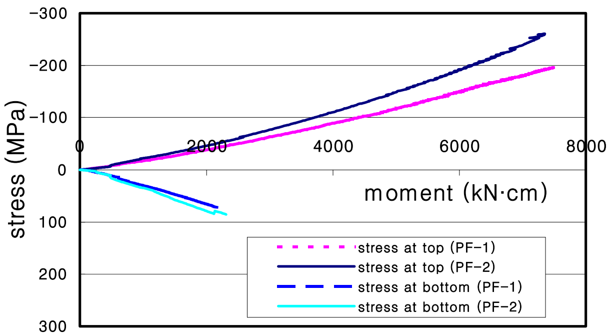

Figure 6. Moment-stress relation at various locations

Table 2. Axial strengths and moments at failure

ID	Axial force (kN)	Axial force at failure (kN)	Moment at failure (kN·cm)
P-1	196	235	9189
P-2	294	337	9265
P-3	588	401	9331
P-4	785	427	9257
P-5	981	578	9867
P-6	1177	1175	6703
P-7	1373	1335	6865

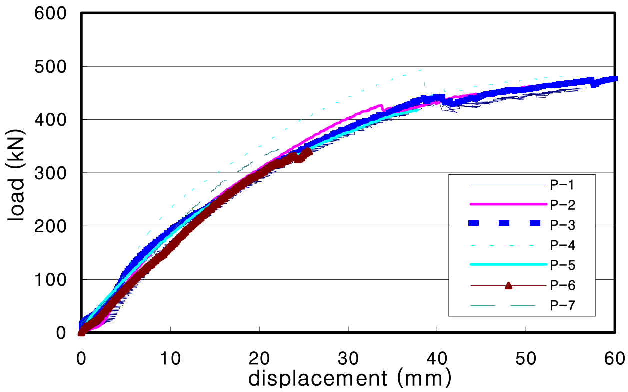

Figure 7. Load-displacement curves at the bottom of mid-span

(a) Tension failure (P-1) (b) Compression failure (P-6)

Figure 8. Photos taken for axial-flexural test at failure

As shown in Figure 8(a), tension failure was occurred for member P-1~P-5. As the load increases the concrete in tension cracks first, then outside tube takes over the moments. Therefore final flexural strength was determined by the yield strength of the glass fibers at the tension side. As shown in Figure 8(b), compression failure was examined at the top surface of test member P-6~P-7 since the larger axial force. Load-strain response curves are drawn in Figure 9. The slopes of the load-displacement curves decrease as the load increases for all test cases. It was confirmed that concrete-filled GFRP tubes show ductile failure for both uni-axial compression and axial-flexure load cases.

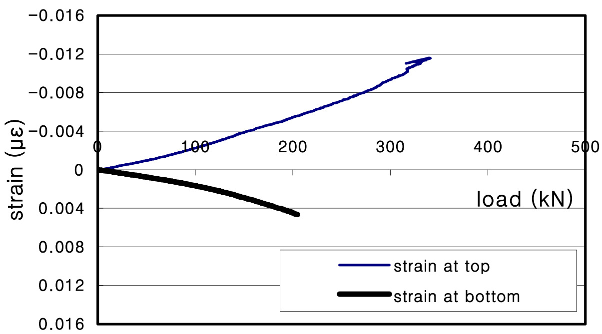

Figure 9. Load-strain curve (P-6)

Prediction of compression behavior using Samaan's model

The bilinear response of GFRP confined concrete can be represented by a relation given by the following equation[7]. n=1.5 and other notations in this equation are given in Figure 10.

By conducting some separate tube test, the first and second slopes of the stress-strain curve in Figure 10 can be obtained. By varying fiber volume, a series of stress-strain relations are obtained as in Figure 11. Based on theses experimental results, the relation between elastic modulus ratio and stiffness ratio was calculated as shown in Figure 12.

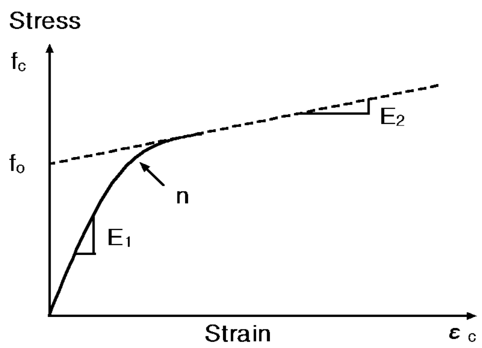

$$f_c = \frac{(E_1 - E_2)\varepsilon_c}{\left[1 + \left(\frac{(E_1 - E_2)\varepsilon_c}{f_0}\right)^n\right]^{1/n}} + E_2\varepsilon_c$$

Figure 10. Constitutive model for FRP-encased concrete (Samaan et al., 1998)

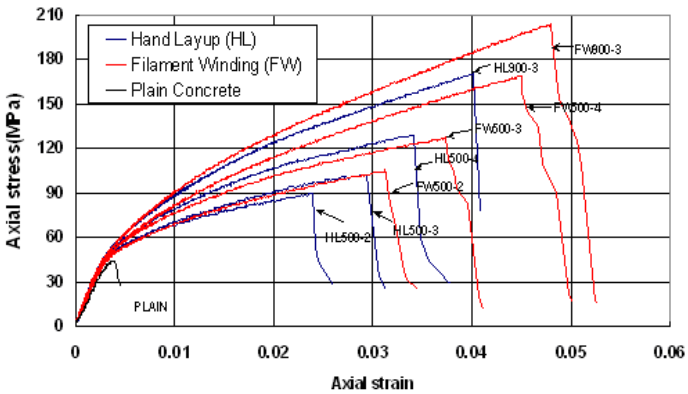

Figure 11. Stress-strain relations obtained by varying tube thickness

The compressive behavior shown in Figure 3 is compared with the current analytical prediction, and the comparison is made in Figure 13.

P-M interaction diagram

A P-M interaction diagram is developed using a simple theoretical computation based on the tensile strength of fibers and compressive response of confined concrete. Computed axial and flexural strength were 96% and 105% of the test results giving good agreement as shown in Figure 13.

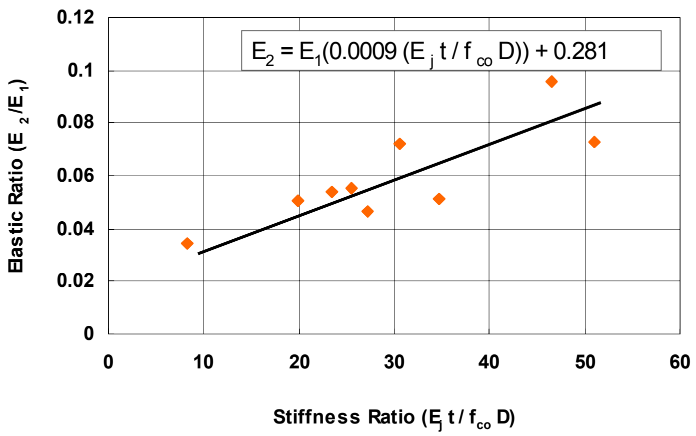

Figure 12. The relation between elastic modulus ratio and stiffness ratio

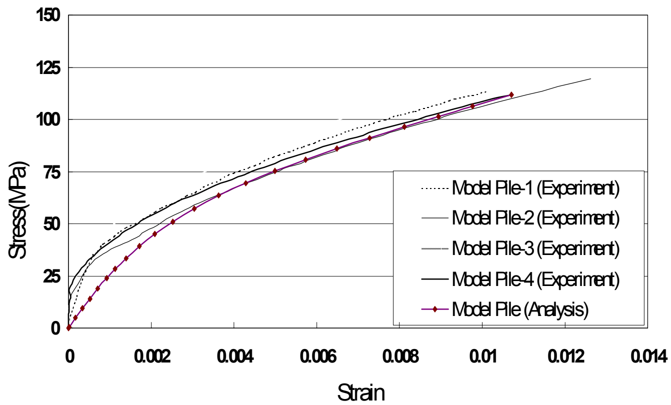

Figure 13. Predicted stress-strain relation compared with test results shown in Figure 3

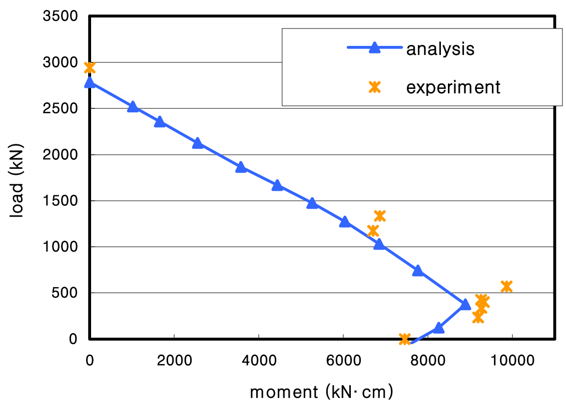

Figure 14. Computed P-M interaction diagram and experimental results

Buckling test

The compressive behavior of slender piles was examined using various slenderness ratios. Four different slenderness ratios (6.7, 14.3, 21.8, and 29.4) were used. Fabrication method for shells is the same as used in the previous experiments. Total 8 GFRP piles were prepared for this buckling test, and all members were loaded with the same strain rate. Design strength for the encased concrete was 27MPa. Failure occurred at the compression zone of the middle surface of the specimen in all test members. Figure 15 shows the typical failure pattern of the pile.

(λ=6.7) (λ=14.3) (λ=21.8) (λ=29.4)

Figure 15. Typical failure pattern of a pile under buckling test

Figure 16 represents the stress-strain curves. Strains were calculated based on the relative displacements between upper and lower loading platens. When the specimens were short, failure was initiated by tensile fracture of shells. On the other hand, compressive failure represents the behavior with slender piles. With high slenderness ratios, strength of the piles and ductility were decreased as shown in Figure 17, and slender piles cannot fully utilize the strength increase obtained by the confinement. Figure 17 reveals the strength of test members reflecting the reduction of values according to the slenderness ratios. In this figure, notation 300_1 means that the pile length is 300mm and 1 represents the specimen ID.

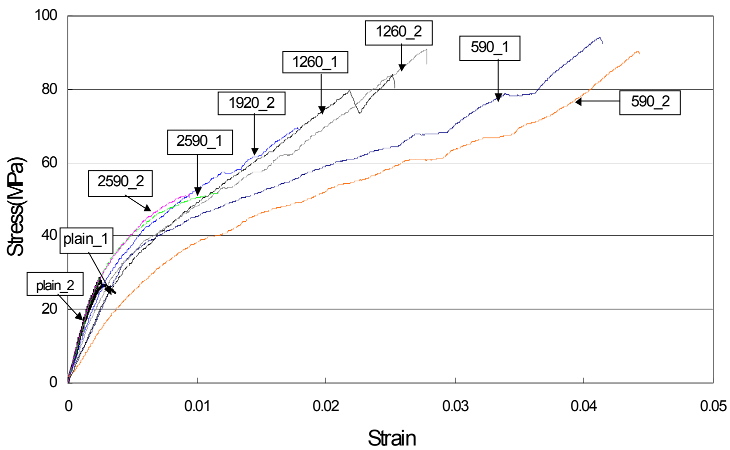

Figure 16. Stress-strain responses of piles

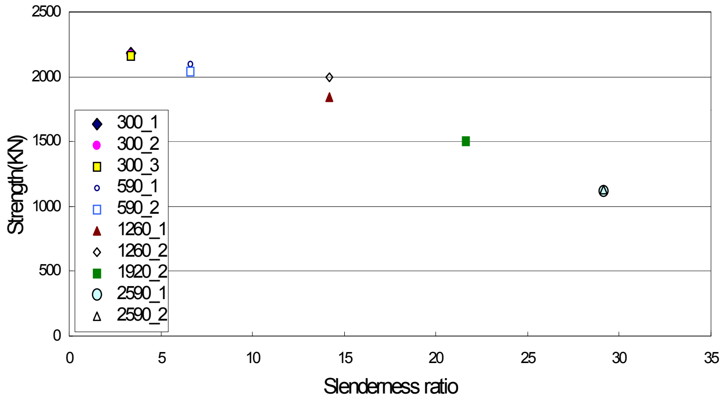

Figure 17. Strength of piles in terms of slenderness ratios

Flexural test for large scale piles

In order to understand the behavior of piles with practical sizes, test piles with inner diameter of 400mm were fabricated for testing. Two different types of piles were made; case L1 piles have 6.7mm tube thickness, and case L2 piles have 9.6mm tube thickness. Four specimens were prepared following case L1; 2 with spirals inside, and 2 without spirals.

Spirals were formed inside in order to verify the effect of bond. For case L2, two specimens which include spirals were fabricated. The same mix design applied for buckling test was used again for this test. Piles were loaded under displacement control with the loading rate of 4 mm/min. Figure 18 shows the testing setup. Displacements were measured at the mid-bottom of the specimen. As shown in the load-displacement curves(Figure 19), performance increases dramatically with spirals. When specimens do not have spirals inside, core concrete were slipped out as load increases, and failure occurred at the compression side of the tube. When spirals were fabricated, the compressive failure of the shell was observed first and then followed by the final tensile failure. In this case, the bond between concrete and shell did not allow slippage and increased the flexure stiffness as shown.

Figure 18. Experimental setup for large scale pile test

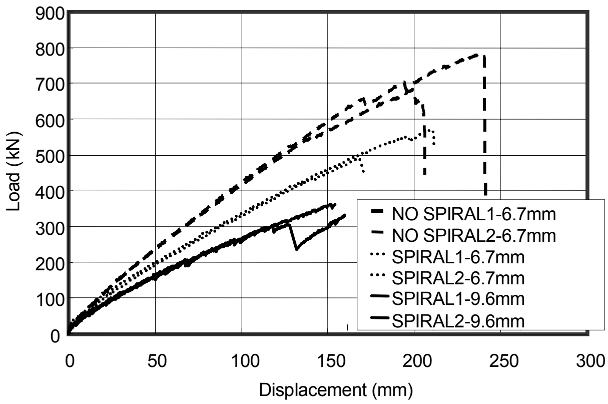

Figure 19. Load-displacement curves of test piles

Conclusions

Structural characteristics of concrete-filled GFRP composite piles were studied in this study. Current research verified the potentiality of concrete-filled composite compression members as an alternative to conventional compression members in corrosive environments, and provides an experimental database for FRP composite piles that are externally reinforced by multidirectional fiber composites. Following conclusions may be drawn.

1) The axial strength of the concrete-filled GFRP tubes increases by a large amount due to the confinement effect given to concrete by the FRP shell.

2) As the flexural load increases, the slope of load-displacement curve decreases and approaches to a very small value at failure. Very ductile failure was observed for both pure axial compression and axial-flexure load.

3) P-M interaction diagram was constructed based on the confined model of encased concrete, and pretty good prediction was obtained.

4) When piles have high slenderness ratios, strength of the piles and ductility were decreased and also cannot fully utilize the strength gained by the confinement effect.

5) The role of bond between encased concrete and shell is essential to guarantee perfect integrity and increased the flexure performance of piles.

Further works necessary include systematic design procedure for the composite tube, precise prediction for bond characteristics, long term behavior of encased concrete, and other application dependent factors.

Acknowledgements

The research presented in this paper was sponsored by the Ministry of Maritime Affairs and Fisheries of Korea, and its support is gratefully acknowledged.

References

[1] Mirmiran, A., “FRP-Concrete Composite Column and Pile Jacket Splicing-Phase II”, Final Report, *Florida DOT,* Tallahassee, Fla., 1997

[2] Mirmiran, A., Shahawy, M. and Samaan, M., “Behavior of Concrete Columns by Fiber Composite”, *J. Struc. Engrg.*, ASCE, Vol. 124, No. 5, 1997, pp. 583-590

[3] Mirmiran, A., Shahawy, M., and Samaan, M. (1999), "Strength and ductility of hybrid FRP-concrete beam columns." *J. Struct. Engrg*., ASCE, 125(10), 1085-1093
[4] Mirmiran, A., Shahawy, M., EI Khoury, C., and Naguib, W. (2000). "Large beam-column tests on concrete-filled composite tubes." *ACI Structural Journal*., 97(2), 268-276
[5] Amir Z. Fam and Sami H. Rizkalla (2001), "Behavior of axially loaded concrete-filled circular fiber reinforced polymer tubes." *ACI Materials Journal*, May-June, 280-289
[6] Lee, S.W. et al. (2002). "Development of Composite Marine Piles of High Durability," *Research Report KMU/SSRC-02/01*, Structural Safety Research Center, Kookmin University, Seoul, Korea
[7] Samaan, M., Mirmiran, A., and Shahawy, M. (1998). "Model of concrete confined by fiber composites." *J. Struct. Engrg*., ASCE, 124(9), 1025-1031.